Node Isolation Probability for Serial Ultraviolet UV-C Multi-hop Networks

Alexander Vavoulas, Harilaos G. Sandalidis, and Dimitris Varoutas

***Abstract*—Non-line-of-sight optical wireless transmission, operated in the unlicensed ultraviolet UV-C band, has been recently suggested as an alternative means of communication. However, due to limited coverage, relayed UV-C networks need to be deployed in order to supply communication services at large distances. In this paper, we consider a serial multi-hop UV-C network where the nodes are distributed at fixed positions on a given service interval. We adopt a suitable path loss model and derive analytical expressions for the node isolation probability assuming on–off keying and pulse position modulation formats. Moreover, we investigate the node density required to achieve connectivity for several geometrical transceiver configurations. The numerical results of this paper are of significant value for telecom researchers working toward a flexible UV-C network deployment in practice.**

***Index Terms*—Multi-hop networks; Node isolation probability; Non-line-of-sight (NLOS) propagation; Ultraviolet (UV-C) transmission.**

I. Introduction

The remarkable channel characteristics of the ultraviolet UV-C spectral region, particularly in the solar-blind band between 200 and 280 nm, have recently enabled the deployment of short range optical wireless communications with non-line-of-sight (NLOS) propagation links. This occurs as the solar-blind region is characterized by both limited background solar radiation and strong atmospheric scattering effects [1,2]. Such technology meets both commercial and military application needs and may be used in the future to alleviate congestion of the radio frequency spectrum in very densely populated areas [3]. However, NLOS UV-C transmitters (Txs) have a limited transmission range of the order of a few tens of meters [4]. Therefore, the deployment of a network by means of multiple node-to-node hops is the key point toward the provision of communication services at large distances.

Transmission through relays is quite a common practice in wireline and RF wireless communication systems. A plethora of such relevant studies has appeared recently; see, e.g., the newly published books of Uysal [5] or Dohler and Li [6]. This technique was also proposed to enhance free space optics (FSO) transmission by mitigating various impairments such as scintillation effects [7]. Very recently, a performance analysis of serial relayed UV-C links has been presented by He *et al.* [8], in order to decrease the transmitter power consumption[1] and the number of LEDs required, extending, thus, the communication range.

Multi-hop networks can properly operate if connectivity between their nodes is satisfied. A fully connected network contains a path from any node to another. When there is no path between at least one source–destination pair, the network is disconnected. In this vein, the node isolation probability can be defined as the probability that a random node cannot communicate with any other nodes [10]. Obviously, connectivity plays a critical role for wireless networking. Some of the studies on this topic for one-dimensional relayed networks are as follows. In [11], the probability of having a wireless network composed of at most C clusters is extracted. In [12], an ad hoc network consisting of nodes and base stations is considered, and the probability of node to base station connectivity is derived. Analytical expressions for the probability that a wireless network is connected are presented in [13], as well. Finally, Miorandi and Altman [14] obtained exact results for the coverage probability, the node isolation probability, and the connectivity distance for various node placement statistics.

Connectivity issues for NLOS UV-C two-dimensional networks deployed in a service area have been discussed in [15]. In that paper, we considered a configuration where transceivers face vertically upwards, that is with a 90° apex angle. Different configurations of receivers (Rxs) and Txs can, however, improve the reliability of UV-C links. These network configurations depend mainly on the Tx divergence angle and Rx field-of-view (FOV). By adjusting the above parameters, one may extend the transmission range to a few meters and achieve an adequate data transfer rate [3].

In the present study, we focus on the node isolation probability evaluation of a serial multi-hop UV-C network and derive analytical expressions assuming the most fundamental modulation formats, i.e., on–off keying (OOK) and pulse position modulation (PPM). The nodes are placed at fixed positions on a given interval and a realistic path loss model is adopted. Such a network can be deployed to provide

[1] The skin and eye exposure limits in the UV-C region, for both continuous and time-limited exposure, were recently established in [9], and the commercial deployment of such a network should be consistent with them. Moreover, it must be noted that under NLOS operation the Txs are facing upwards, thus eliminating direct human exposure to UV radiation.

Manuscript received March 17, 2011; revised July 15, 2011; accepted July 15, 2011; published August 30, 2011 (Doc. ID 144262).

Alexander Vavoulas is with the Department of Informatics and Telecommunications, University of Athens, Panepistimiopolis, GR-15784 Athens, Greece, and is also with the Department of Computer Science and Biomedical Informatics, University of Central Greece, Papasiopoulou 2–4, GR-35100 Lamia, Greece.

Harilaos G. Sandalidis (e-mail: sandalidis@hotmail.com) is with the Department of Computer Science and Biomedical Informatics, University of Central Greece, Papasiopoulou 2–4, GR-35100 Lamia, Greece.

Dimitris Varoutas is with the Department of Informatics and Telecommunications, University of Athens, Panepistimiopolis, GR-15784 Athens, Greece.

Digital Object Identifier 10.1364/JOCN.3.000750

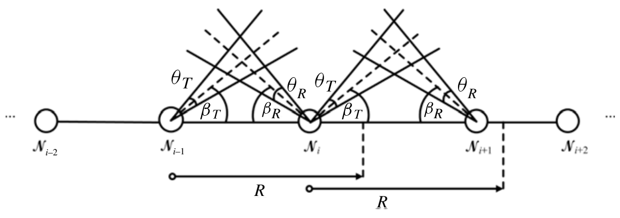

Fig. 1. Serial UV-C multi-hop network geometry.

communication services, for example, alongside a railroad or a motorway. Several illustrative examples are presented to show the interaction between various parameters, including the node density, the data rate, the required amount of power to achieve a certain error probability floor, etc. Moreover, different geometrical transceiver characteristics are considered in order to find the node density value which avoids the possibility of nodes becoming isolated.

The remainder of the paper is organized as follows. Section II presents, in brief, the assumptions followed by the network model. It also summarizes the fundamental concepts of the node isolation probability assuming that the nodes are distributed following a one-dimensional Poisson point process (PPP). The UV-C path loss model is described and analytical expressions of the achievable ranges for the OOK and PPM modulation schemes are deduced as well. Numerical results are illustrated and discussed in Section III. Finally, some concluding remarks are given in Section IV.

II. Network Concepts

A. UV-C Network Model

The UV-C network model follows the configuration shown in Fig. 1. The network consists of n transceivers (nodes), deployed at fixed positions on a service interval with length ℓ, operating under NLOS conditions. Every node is independently placed on the service interval according to a homogeneous one-dimensional PPP. Assuming large values of n and ℓ, a constant node density, $\rho = n/\ell$, can be obtained. Under this assumption, the homogeneous PPP can be obtained as the limiting case of the uniform distribution [16]. The homogeneous PPP has a central role in point process statistics since it is the simplest and most important infinite point process model. However, more complicated models can be obtained for specialized scenarios. For instance, the nodes may occur in clusters or may exhibit regularity. Furthermore, there may be a hard-core distance, i.e., a distance D_0 around each node where no other nodes are located [17].

Every node is equipped with a Tx and a Rx, with elevation angles of β_T and β_R degrees, respectively. The distance between a transceiver and its first neighbor is a random variable following a generalized Gamma distribution [18]. The Tx produces a cone, which has a beam divergence angle of θ_T degrees, and intersects the Rx FOV cone of θ_R degrees. A communication link is established when the optical power is backscattered by particles inside the common volume, generated by the intersection of the two cones, and reaches the Rx node.

We consider the case of homogeneous range assignment, i.e., all the nodes have the same transmission range $R > 0$ [19]. Every source node forwards traffic toward its first neighbor node provided that their cones are intersected. If this does not happen, the node becomes isolated. If the transmission range is short, the probability of having isolated nodes increases. On the contrary, assuming a large value of R, the interference level for each node may be significantly increased, thus degrading the quality of the communication link. Obviously, an appropriate trade off between the node density, ρ, and the transmission range, R, is required to ensure a minimum number of isolated nodes.

B. Node Isolation Probability

The distance between a node and its mth neighbor for a homogeneous one-dimensional PPP with density ρ is a random variable with probability density function [18]

$$f_{R_m}(r) = \frac{(2\rho r)^m}{r\Gamma(m)} e^{-2\rho r}. \tag{1}$$

A node becomes isolated when its first neighbor is beyond its range R; thus, the node isolation probability, P_{iso}, is given by

$$\begin{aligned} P_{\text{iso}} &= \Pr(r \geqslant R) = 1 - \Pr(0 \leqslant r \leqslant R) \\ &= 1 - \int_0^R \frac{2\rho}{\Gamma(1)} e^{-2\rho r} dr = e^{-2\rho R}. \end{aligned} \tag{2}$$

This result is also consistent with Eq. (13) in [10] for $n_0 = 0$. It is clear that the node isolation probability depends on the node density, ρ, as well as the transmission range, R, of every UV-C node.

The minimum transmission range, ensuring P_{iso} close to zero, is important for the proper operation of the network. As stated in [16], the avoidance of isolated nodes is a necessary but not sufficient condition for a network to be connected. Furthermore, the node density required to avoid isolated nodes with a certain probability is a lower bound for the node density required for a connected network with the same probability [16, Eq. (18)]. However, the minimum transmission range is directly related to the adopted modulation and/or coding format. Therefore, assuming a homogeneous range assignment, R, for a given modulation scheme, the study derives the minimum node density, ρ, required to achieve a network with node isolation probability close to zero.

C. Path Loss Model

We assume a homogeneous atmosphere characterized by the Rayleigh (molecular) scattering coefficient k_s^{Ray}, the Mie (aerosol) scattering coefficient k_s^{Mie}, the absorption coefficient k_a, and the extinction coefficient k_e. The turbulence effects are in general negligible since the distances between the nodes are quite short. The total scattering coefficient is the sum of the two scattering coefficients, $k_s = k_s^{\text{Ray}} + k_s^{\text{Mie}}$.

TABLE I
SYSTEM MODEL PARAMETERS ([2,20])

Parameter	Value
Wavelength λ	260 nm
Tx average power P_t	50 mW
Tx elevation angle β_T	30°
Rx elevation angle β_R	30°
Tx beam full-width divergence θ_T	10°
Rx FoV angle θ_R	10°
Noise photon count rate N_n	14,500 s^{-1}
Photomultiplier tube responsivity ζ	62 A/W
Optical filter efficiency η_f	0.15
Photomultiplier tube quantum efficiency η_{PMT}	0.30
Probability of error P_e	10^{-3}
Data rate R_b	100 kbps
Length of PPM symbol M	4
Area of receiving aperture A_r	$1.77 \cdot 10^{-4}$ m^{-2}
Absorption coefficient k_a	$0.9 \cdot 10^{-3}$ m^{-1}
Mie scattering coefficient k_s^{Mie}	$0.25 \cdot 10^{-3}$ m^{-1}
Rayleigh scattering coefficient k_s^{Ray}	$0.24 \cdot 10^{-3}$ m^{-1}
γ	0.017
g	0.72
f	0.5

The extinction coefficient is the sum of the scattering and absorption coefficients, i.e., $k_e = k_s + k_a$. The scattering atmosphere is characterized by the composite phase function, $P(\mu)$, as suggested in [20]:

$$P(\mu) = \frac{P_{\text{Ray}}(\mu) + (k_s^{\text{Mie}}/k_s^{\text{Ray}})P_{\text{Mie}}(\mu)}{1 + (k_s^{\text{Mie}}/k_s^{\text{Ray}})}, \tag{3}$$

where $\mu = \cos\beta_s$, $\beta_s = \beta_R + \beta_T$ is the scattering angle, and $P_{\text{Ray}}(\mu)$ and $P_{\text{Mie}}(\mu)$ are the phase functions modeled by a generalized Rayleigh model and a generalized Henvey–Greenstein function, respectively, given by [21] and [20], accordingly:

$$P_{\text{Ray}}(\mu) = \frac{3[1 + 3\gamma + (1-\gamma)\mu^2]}{16\pi(1+2\gamma)}, \tag{4}$$

$$P_{\text{Mie}}(\mu) = \frac{1-g^2}{4\pi}\left[\frac{1}{(1+g^2-2g\mu)^{3/2}} + f\frac{0.5(3\mu^2-1)}{(1+g^2)^{3/2}}\right], \tag{5}$$

where γ, g, and f are model parameters.

The determination of an appropriate path loss model is an open issue in the technical literature. As an example, Chen *et al.* in [22] suggested an empirical model based on experimental measurements for various apex angles and fixed Tx divergence angles and Rx FOV. Here, we adopt a single scattering model, where each photon is assumed to be scattered at most once through its propagation from Tx to Rx. This model has been derived by Xu *et al.* in [21], as a fine approximation of the one introduced by Luettgen *et al.* in [23], which is presented in an integral form. Xu's path loss model is given as

$$L \approx \frac{96R\sin\beta_T \sin^2\beta_R\left(1-\cos\frac{\theta_T}{2}\right)\exp\left(\frac{k_e R\beta_1}{\sin\beta_s}\right)}{k_s P(\mu)A_r\theta_T^2\theta_R\sin\beta_s(12\sin^2\beta_R + \theta_R^2\sin^2\beta_T)}, \tag{6}$$

where $\beta_1 = \sin\beta_T + \sin\beta_R$ and A_r is the area of the receiving aperture.

D. Minimum Transmission Range

The minimum achievable transmission range of each node depends on the adopted modulation format.

For the OOK scheme, the relationship between the minimum required transmitted power, P_t, and the achieved probability of error, P_e, assuming a Gaussian noise model, is given by [24]

$$\frac{\eta P_t}{L} = \sqrt{N_0 R_b}\,Q^{-1}(P_e), \tag{7}$$

where L is the path loss, η is the quantum efficiency of the optical filter and photodetector, R_b is the data rate, $Q(\cdot)$ is the Gaussian Q function defined as $Q(x) = 1/\sqrt{2\pi}\int_x^\infty \exp^{-\frac{t^2}{2}}dt$ and also related to the complementary error function erfc(·) by $\text{erfc}(x) = 2Q(\sqrt{2}x)$, and

$$N_0 = \frac{q\zeta N_n hc}{\lambda} \tag{8}$$

is the white noise power spectral density. In Eq. (8), q denotes the electrical charge, ζ is the photomultiplier tube responsivity, N_n is the noise photon count rate, h is Planck's constant, λ is the wavelength, and c is the speed of light. The minimum transmission range for OOK, R_{OOK}, is obtained by substituting the variable L of Eq. (7) by its value given by Eq. (6) and solving for R. The result is given in Eq. (9) (see Box 1), where $W_0(\cdot)$ denotes the principal real-valued branch of the Lambert W function.[2]

For the PPM format, the relationship between the minimum required transmitted power, P_t, and the achieved probability of error, P_e, assuming a Gaussian noise model, is given by [24]

$$\frac{\eta P_t}{L} = \sqrt{\frac{2N_0 R_b}{M\log_2 M}}\,Q^{-1}(P_e), \tag{10}$$

where M is the length of the PPM symbol. Similarly, the minimum transmission range, R_{PPM} is given by Eq. (11) (see Box 2).

Therefore, we can find an analytical expression for the node isolation probability, P_{iso}, by substituting the variable R of Eq. (2) by the value given by Eq. (9) (see Box 1) or or Eq. (11) (see Box 2), in terms of the system parameters (i.e., transmitted power, supported data rate, and probability of error), as well as the geometrical configuration parameters (i.e., Tx and Rx elevation angles, Tx full beam divergence angle, and Rx FOV), and the node density.

III. NUMERICAL RESULTS AND DISCUSSION

In this section, numerical results are presented for a set of model parameters given in Table I. These parameters are kept constant, unless specified otherwise.

Figures 2(a)–2(d) demonstrate the impact of the system parameters on the node isolation probability assuming OOK.

[2] The Lambert W function is defined as the solution of the equation $ye^y = x$. That is $W(x) = y$. It is noted that the Lambert function is implemented in some mathematical software, e.g., see the function ProductLog in [25].

$$R_{\mathrm{OOK}} = \frac{\sin\beta_s}{k_e\beta_1} W_0\left(\frac{\eta P_t k_s P(\mu) A_r \theta_T^2 \theta_R k_e \beta_1 (12\sin^2\beta_R + \theta_R^2 \sin^2\beta_T)}{96\sin\beta_T \sin^2\beta_R \left(1-\cos\frac{\theta_T}{2}\right)\sqrt{N_0 R_b}\,Q^{-1}(P_e)}\right) \tag{9}$$

Box 1.

$$R_{\mathrm{PPM}} = \frac{\sin\beta_s}{k_e\beta_1} W_0\left(\frac{\eta P_t k_s P(\mu) A_r \theta_T^2 \theta_R \sqrt{M\log_2 M}\, k_e \beta_1 (12\sin^2\beta_R + \theta_R^2 \sin^2\beta_T)}{96\sin\beta_T \sin^2\beta_R \left(1-\cos\frac{\theta_T}{2}\right)\sqrt{2N_0 R_b}\,Q^{-1}(P_e)}\right) \tag{11}$$

Box 2.

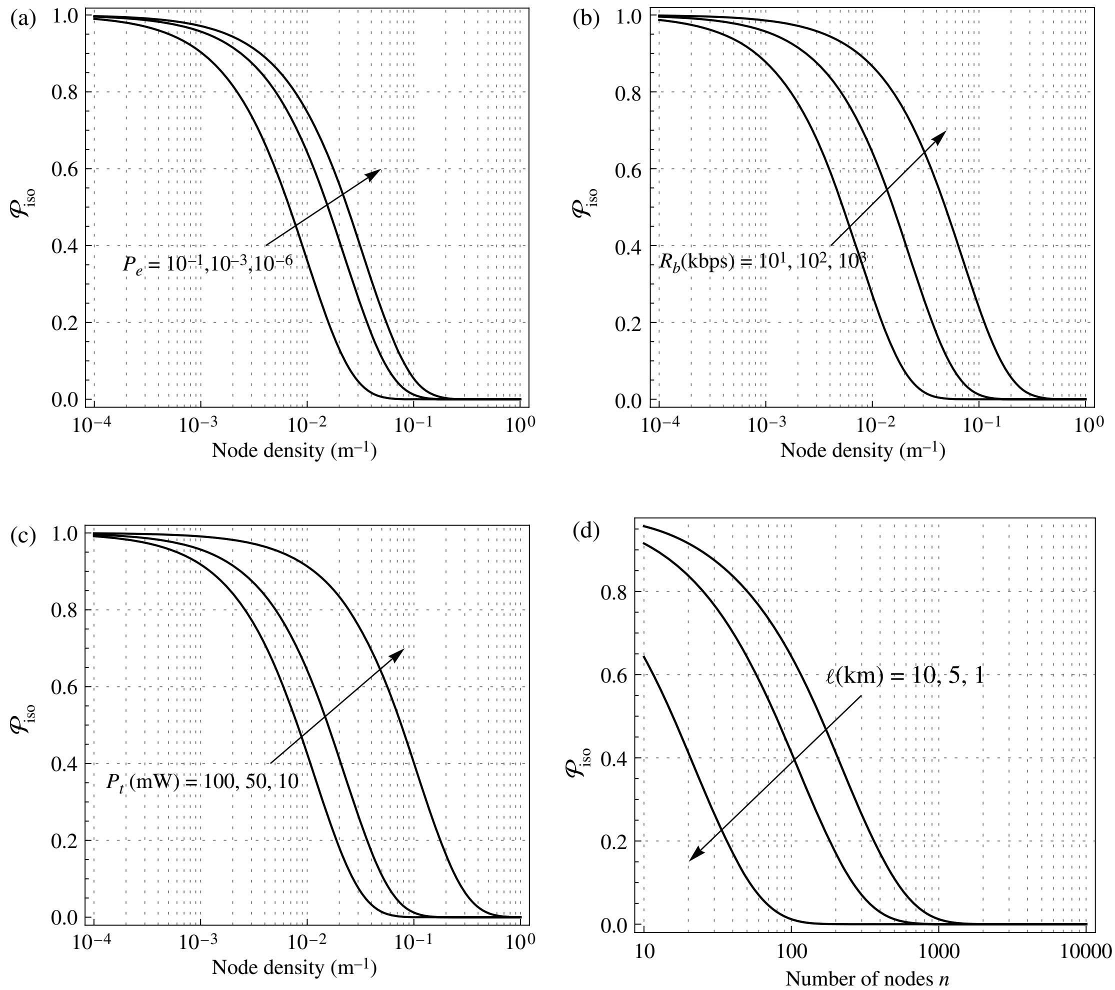

Fig. 2. P_{iso} versus (a) node density, ρ, for various values of P_e, (b) node density, ρ, for various values of R_b, (c) node density, ρ, for various values of P_t, and (d) number of nodes, n, for various lengths, ℓ, of service interval assuming OOK modulation.

First, in Fig. 2(a), we observe that as P_e increases, the node density required to achieve a node isolation probability close to zero decreases. Moreover, an increase of the data rate by a factor equal to 10 demands a 3.5 times denser node distribution to preserve network stability according to Fig. 2(b). The impact of transmitted power is dominant, as shown in Fig. 2(c), since the reduction of P_t from 100 to 50 mW demands a double node density, whereas a further reduction to 10 mW induces a

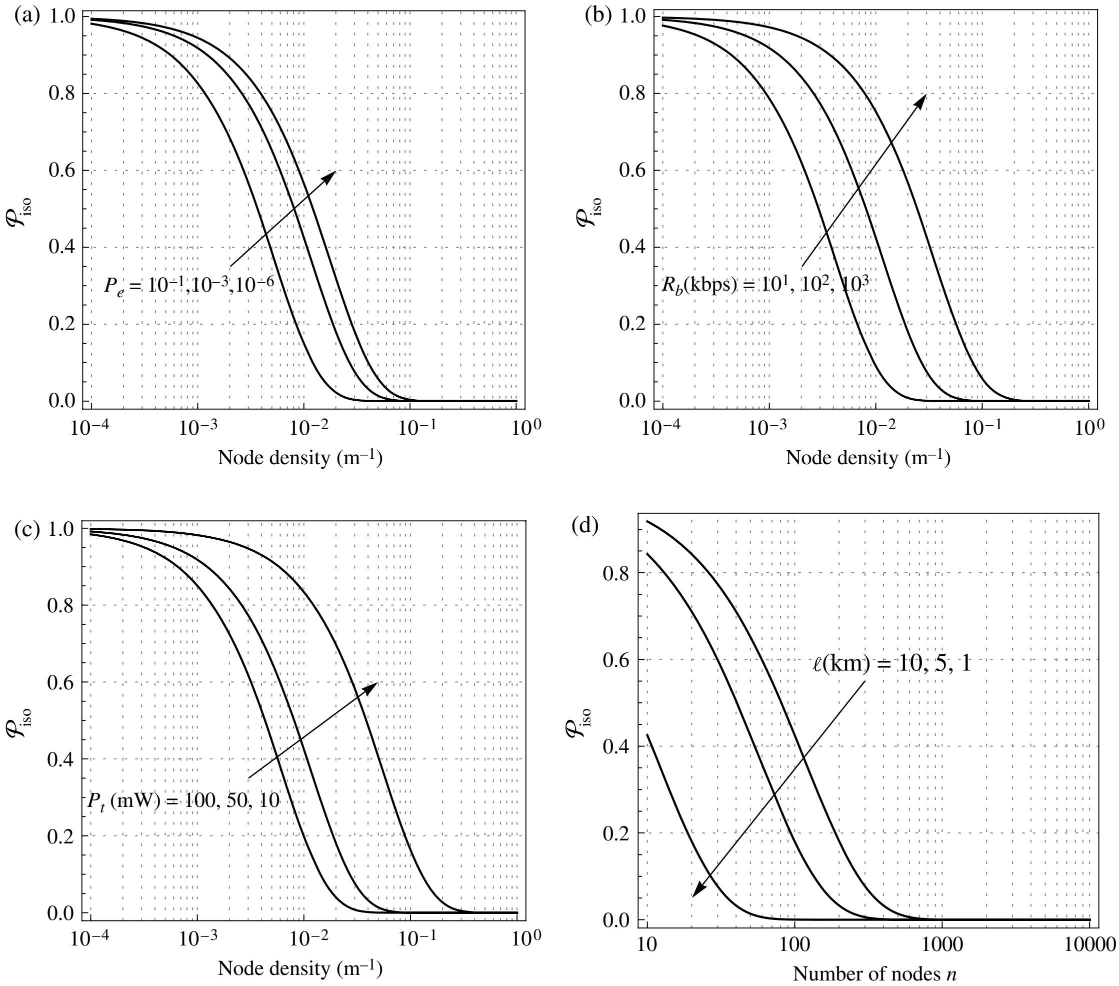

Fig. 3. P_{iso} versus (a) node density, ρ, for various values of P_e, (b) node density, ρ, for various values of R_b, (c) node density, ρ, for various values of P_t, and (d) number of nodes, n, for various lengths, ℓ, of service interval assuming PPM modulation.

fivefold node density. Finally, the trade-off between the number of nodes required to cover a service interval of specific length ℓ is illustrated in Fig. 2(d). Assuming $P_e = 10^{-3}$, $R_b = 100$ kbps, and $P_t = 50$ mW, we need $n = 150$, 800, and 1400 nodes to cover service intervals with lengths $\ell = \{1, 5, 10\}$ km, respectively.

Similar results for the PPM scheme are shown in Figs. 3(a)–3(d). Here, to cover service intervals with lengths $\ell = \{1, 5, 10\}$ km, as depicted in Fig. 2(d), we need $n = 70$, 370, and 700, accordingly, under the same assumptions for P_e, R_b, and P_t. By comparing Figs. 2 and 3, we observe that the required node density to achieve a node isolation probability close to zero is significantly smaller by adopting the PPM format. Furthermore, we observe that we need half as many nodes to cover the same service length in comparison with the OOK scheme. It is clear that the adoption of a more effective modulation and/or coding scheme may significantly reduce the number of the nodes required to cover an interval with a specific length.

Figures 4–7 illustrate the node density, ρ, required to achieve $P_{\text{iso}} \approx 0$ against the Tx and Rx geometry for the OOK and PPM schemes, respectively. We assume constant values of P_e, R_b, and P_t according to Table I. In Figs. 4 and 6 we observe that the required node density for a specific value set of $\{\beta_T, \beta_R\}$, considering the PPM scheme, is almost half of the

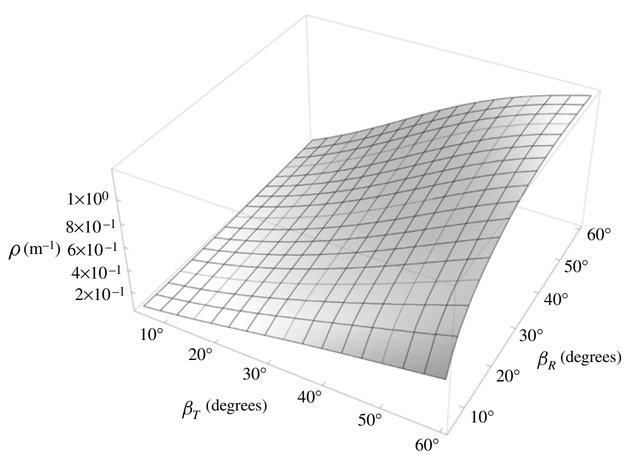

Fig. 4. Required node density, ρ, to achieve $P_{\text{iso}} \approx 0$ versus elevation angles β_T and β_R assuming $P_t = 50$ mW, $R_b = 100$ kbps, $P_e = 10^{-3}$, $\theta_T = 10°$, $\theta_R = 10°$, and OOK modulation.

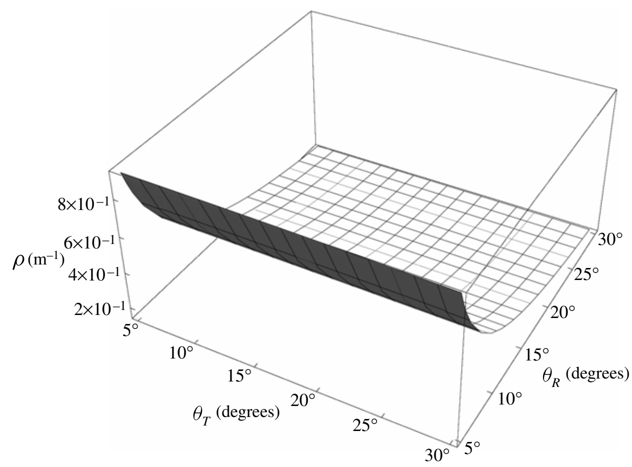

Fig. 5. Required node density, ρ, to achieve $P_{\text{iso}} \approx 0$ versus Tx beam divergence angle θ_T and Rx FOV θ_R assuming $P_t = 50$ mW, $R_b = 100$ kbps, $P_e = 10^{-3}$, $\beta_T = 30°$, $\beta_R = 30°$, and OOK modulation.

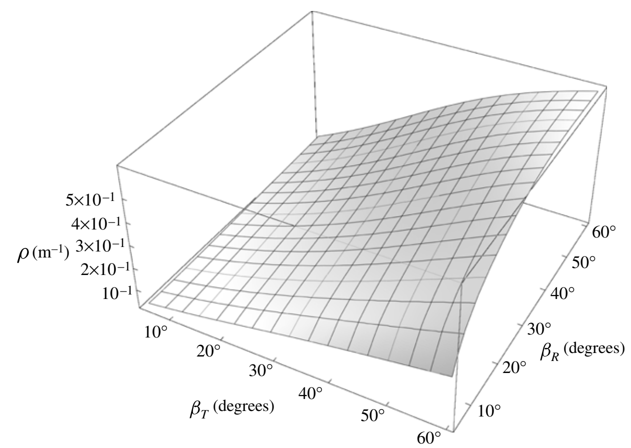

Fig. 6. Required node density, ρ, to achieve $P_{\text{iso}} \approx 0$ versus elevation angles β_T and β_R assuming $P_t = 50$ mW, $R_b = 100$ kbps, $P_e = 10^{-3}$, $\theta_T = 10°$, $\theta_R = 10°$, and PPM modulation.

corresponding one for the OOK scheme. The same remark is observed by comparing Figs. 5 and 7 for the same value set of $\{\theta_T,\ \theta_R\}$. Furthermore, we observe that the required node density is reduced as the values of $\{\beta_T,\ \beta_R\}$ decrease. This is anticipated, since smaller elevation angles increase the range of each node. In Fig. 5, we can see the dominant impact of the Rx FOV on the network robustness. It is clear that as the Rx FOV decreases, fewer photons may reach the receiver and lower optical power is collected, so a denser network is required. It is worth mentioning that as the Tx beam divergence angle and Rx FOV become wide, the positioning of Tx and Rx becomes less important. In any case, these results are a valuable tool toward a flexible UV-C network deployment.

IV. Conclusions

Transmission through relays is quite a common practice in wireline and wireless communications in order to provide services at large distances. This technique is even more

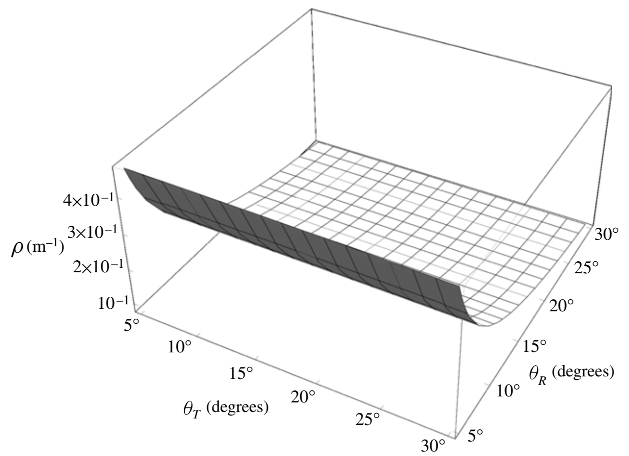

Fig. 7. Required node density, ρ, to achieve $P_{\text{iso}} \approx 0$ versus Tx beam divergence angle θ_T and Rx FOV θ_R assuming $P_t = 50$ mW, $R_b = 100$ kbps, $P_e = 10^{-3}$, $\beta_T = 30°$, $\beta_R = 30°$, and PPM modulation.

important in the case of UV-C communication systems due to their limited transmission range. Multi-hop UV-C networks operate properly if their nodes are not isolated.

In this paper, we presented analytical expressions for the node isolation probability of a serial NLOS UV-C network where transceivers are distributed statistically on a given service interval. We used an effective path loss model and considered transmission with both OOK and PPM modulation schemes assuming Gaussian noise. Several illustrative examples were depicted to show the interaction between various parameters, including the node density, the data rate, the required amount of power to achieve a certain error probability floor, etc. Different geometrical transceiver configurations were examined in order to obtain the node density required to achieve $P_{\text{iso}} \approx 0$ as well.

The obtained results can be useful for designers to predict and evaluate a UV-C network's ability to deliver communication services in real conditions. For instance, assuming a service length of 10 km and typical values of transmitted power, probability of error, and supported data rate, according to Table I, we find from Figs. 2(d) and 3(d) that approximately 1400 nodes for OOK and 700 nodes for PPM are necessary to deploy a fully connected serial multi-hop UV-C network. The adoption of other path loss models and the consideration of more effective modulation and/or coding schemes are some of the topics for further research.

References

[1] D. M. Reilly, D. T. Moriarty, and J. A. Maynard, “Unique properties of solar blind ultraviolet communication systems for unattended ground sensor networks,” *Proc. SPIE*, vol. 5611, pp. 244–254, Nov. 2004.

[2] G. A. Shaw, M. L. Nischan, M. A. Iyengar, S. Kaushik, and M. K. Griffin, “NLOS UV communication for distributed sensor systems,” *Proc. SPIE*, vol. 4126, pp. 83–96, Nov. 2000.

[3] Z. Xu and B. M. Sadler, “Ultraviolet communications: Potential and state-of-the-art,” *IEEE Commun. Mag.*, vol. 46, no. 5, pp. 67–73, May 2008.

[4] D. Keddar and S. Arnon, "Non-line-of-sight optical wireless sensor network operating in multiscattering channel," *Appl. Opt.*, vol. 45, no. 33, pp. 8454–8461, Nov. 2006.

[5] M. Uysal, Ed., *Cooperative Communications for Improved Wireless Network Transmission: Framework for Virtual Antenna Array Applications*. Information Science Reference, 2010.

[6] M. Dohler and Y. Li, *Cooperative Communications: Hardware, Channel and PHY*. Wiley, 2010.

[7] G. K. Karagiannidis, T. A. Tsiftsis, and H. G. Sandalidis, "Outage probability of relayed free space optical communication systems," *Electron. Lett.*, vol. 42, no. 17, pp. 994–995, Aug. 2006.

[8] Q. He, Z. Xu, and B. M. Sadler, "Non-line-of-sight serial relayed link for optical wireless communications," in *IEEE Military Communications Conf.*, San Jose, CA, 31 Oct.–3 Nov. 2010, pp. 1588–1593.

[9] The International Commission on Non-Ionizing Radiation and Protection (ICNIRP), "Guidelines on limits of exposure to ultraviolet radiation of wavelengths between 180 nm and 400 nm (incoherent optical radiation)," *Health Phys.*, vol. 87, no. 2, pp. 171–186, Aug. 2004.

[10] C. Bettstetter, "On the minimum node degree and connectivity of a wireless multihop network," in *Proc. ACM MobiHoc*, Lausanne, Switzerland, 9–11 June 2002, pp. 80–91.

[11] A. Ghasemi and S. Nader-Esfahani, "Exact probability of connectivity in one-dimensional ad hoc wireless networks," *IEEE Commun. Lett.*, vol. 10, no. 4, pp. 251–253, Apr. 2006.

[12] A. Behnad and S. Nader-Esfahani, "Probability of node to base station connectivity in one-dimensional ad hoc networks," *IEEE Commun. Lett.*, vol. 14, no. 7, pp. 650–652, July 2010.

[13] M. Desai and D. Manjunath, "On the connectivity in finite ad hoc networks," *IEEE Commun. Lett.*, vol. 6, no. 10, pp. 437–439, Oct. 2002.

[14] D. Miorandi and E. Altman, "Connectivity in one-dimensional ad hoc networks: A queueing theoretical approach," *Wireless Networks*, vol. 12, no. 5, pp. 573–587, Oct. 2006.

[15] A. Vavoulas, H. G. Sandalidis, and D. Varoutas, "Connectivity issues for ultraviolet UV-C networks," *J. Opt. Commun. Netw.*, vol. 3, no. 3, pp. 199–205, Mar. 2011.

[16] C. Bettstetter and C. Hartmann, "Connectivity of wireless multihop networks in a shadow fading environment," *Wireless Networks*, vol. 11, no. 5, pp. 571–579, Nov. 2005.

[17] D. Stoyan, W. S. Kendall, and J. Mecke, *Stochastic Geometry and Its Applications*. Wiley, 1996.

[18] M. Haenggi, "On distances in uniformly random networks," *IEEE Trans. Inf. Theory*, vol. 51, no. 10, pp. 3584–3586, Oct. 2005.

[19] C. Bettstetter, "On the connectivity of wireless multihop networks with homogeneous and inhomogeneous range assignment," in *Proc. IEEE VTC Fall*, Vancouver, BC, Canada, Sept. 24–28 2002, pp. 1706–1710.

[20] A. S. Zachor, "Aureole radiance field about a source in a scattering absorbing medium," *Appl. Opt.*, vol. 17, no. 12, pp. 1911–1922, June 1978.

[21] Z. Xu, H. Ding, B. M. Sadler, and G. Chen, "Analytical performance study of solar blind non-line-of-sight ultraviolet short-range communication links," *Opt. Lett.*, vol. 33, no. 16, pp. 1860–1862, Aug. 2008.

[22] G. Chen, Z. Xu, H. Ding, and B. M. Sadler, "Path loss modeling and performance trade-off study for short-range non-line-of-sight ultraviolet communications," *Opt. Express*, vol. 17, no. 5, pp. 3929–3940, Mar. 2009.

[23] M. Luettgen, J. Shapiro, and D. Reilly, "Non-line-of-sight single-scatter propagation model," *J. Opt. Soc. Am.*, vol. 8, no. 12, pp. 1964–1972, Dec. 1991.

[24] Q. He, B. M. Sadler, and Z. Xu, "Modulation and coding tradeoffs for non-line-of-sight ultraviolet communications," *Proc. SPIE*, vol. 7464, 74640H, Aug. 2009.

[25] *The Wolfram functions site* [Online]. Available: http://functions.wolfram.com.

Alexander Vavoulas was born in Athens, Greece, in July 1976. He received his B.Sc. degree in physics and M.Sc. degree in electronics and radio-communications in 2000 and 2002, respectively, both from the University of Athens, Greece. He is currently working toward a Ph.D. degree at the same university.

Since 2009, he has been a member of the Special and Laboratorial Teaching Staff at the Department of Computer Science and Biomedical Informatics of the University of Central Greece.

His major research interests include physical and MAC layer issues for fixed broadband wireless access systems, optical wireless communications, and technoeconomic evaluation of network services. He serves as a reviewer for several journals and conferences.

Harilaos G. Sandalidis was born in Florina, Greece, in 1972. He received his five-year Diploma degree in electronics and computer engineering and M.Sc. degree in business administration from the Production Engineering and Management Department of the Technical University of Crete, Greece, in 1995 and 1998, respectively. He also received an M.Sc. degree in radiofrequency and microwave communications and a Ph.D. degree in the telecommunications area from the Electronics and Telecommunications (former Electronics and Electrical Engineering) Department of the University of Bradford, UK, in 1996 and 2002, respectively.

During the period between 1996 and 2001 he was a Research Assistant at the Telecommunications Systems Institute of Crete, Greece, working toward his Ph.D. degree in collaboration with the University of Bradford. After his military service, he joined TEMAGON, the technology consulting branch of the Hellenic Telecommunications Organization (OTE Group), in 2002, where he was involved in the risk mitigation program for the 2004 Olympic Telecommunication Network in collaboration with Telcordia Technologies, Inc. He also worked as a Senior Investigator at the Greek Ombudsman's Office. In March 2009 he joined the University of Central Greece, where he is a Lecturer at the Department of Computer Science and Biomedical Informatics.

His major research interests include optical wireless communications, computational intelligence, and heuristic optimization techniques regarding their application to the telecommunications field.

Dimitris Varoutas holds a Physics degree and M.Sc. and Ph.D. diplomas in communications and technoeconomics from the University of Athens. He serves as an Assistant Professor in the Department of Informatics and Telecommunications at the University of Athens. He has participated in numerous European R&D projects in the RACE I&II, ACTS, Telematics, RISI, and IST frameworks in the areas of telecommunications and technoeconomics. He actively participates in several technoeconomic activities for telecommunications, networks, and services such as the ICT-OMEGA and the CELTIC/CINEMA projects, as well as the Conferences on Telecommunications TechnoEconomics. He also participates in or manages related national activities for technoeconomic evaluation of broadband strategies, telecommunications demand forecasting, price modeling, etc. His research interests span design of optical and wireless communications systems to technoeconomic evaluation of network architectures and services. He has published more than

80 publications in refereed journals and conferences in the area of telecommunications, optoelectronics, and technoeconomics, including leading IEEE journals and conferences. He is a member of the IEEE Photonics Society, the Communications, Circuits and Systems, and Education and Engineering Management Societies of IEEE and serves as a reviewer for several, including IEEE, journals and conferences. Since 2007, he has been the Deputy Vice Chairman of ADAE, the National Authority for Communications Security and Privacy.